Published in final edited form as:
Stem Cells. 2010 June ; 28(6): 1060–1070. doi:10.1002/stem.431.

MicroRNA miR-137 regulates neuronal maturation by targeting ubiquitin ligase Mind Bomb-1

Richard D. Smrt[1], **Keith E. Szulwach**[2], **Rebecca L. Pfeiffer**[1], **Xuekun Li**[1], **Weixiang Guo**[1], **Manavendra Pathania**[3], **Zhao-Qian Teng**[1], **Yuping Luo**[1], **Junmin Peng**[2], **Angelique Bordey**[3], **Peng Jin**[2,*], and **Xinyu Zhao**[1,*]

[1]Department of Neurosciences, University of New Mexico School of Medicine, Albuquerque, NM 87131

[2]Department of Human Genetics and Graduate Program in Genetics and Molecular Biology, Emory University School of Medicine, Atlanta, GA

[3]Department of Neurosurgery, Yale School of Medicine, New Haven, CT 06520-8082

Abstract

A final step of neurogenesis is the maturation of young neurons, which is regulated by complex mechanisms and dysregulation of this process is frequently found in neurodevelopmental disorders. MicroRNAs have been implicated in several steps of neuronal maturation including dendritic and axonal growth, spine development, and synaptogenesis. We demonstrate that one brain-enriched microRNA, miR-137, has a significant role in regulating neuronal maturation. Overexpression of miR-137 inhibits dendritic morphogenesis, phenotypic maturation, and spine development both in brain and cultured primary neurons. On the other hand, a reduction in miR-137 had opposite effects. We further show that miR-137 targets the Drosophila Mib1 protein through the conserved target site located in the 3′ untranslated region of *Mib1* mRNA. Mib1 is an ubiquitin ligase known to be important for neurodevelopment. We show that exogenously expressed Mib1 could partially rescue the phenotypes associated with miR-137 overexpression. These results demonstrate a novel miRNA-mediated mechanism involving miR-137 and Mib1 that function to regulate neuronal maturation and dendritic morphogenesis during development.

[*]Correspondence: Xinyu Zhao, Ph.D., Department of Neurosciences, University of New Mexico School of Medicine, Albuquerque, NM 87131, xzhao@salud.unm.edu. Peng Jin, Ph.D., Department of Human Genetics, Emory University School of Medicine, 615 Michael Street, Suite 301, Atlanta, GA 30322, peng.jin@emory.edu.

Conflict of interest

The authors declare that they have no conflict of interest.

Author Contributions:

Richard Smrt: Concept and design, collection and/or assembly of data, data analysis and interpretation, manuscript writing, final approval of manuscript
Keith Szulwach: Collection and/or assembly of data, data analysis and interpretation, final approval of manuscript
Rebecca Pfeiffer: Collection of data
Xuekun Li: Provision of study material
Weixiang Guo: Collection of data
Manavendra Pathania: Collection of data
Zhao-Qian Teng: Collection of data
Yuping Luo: Provision of study material
Junmin Peng: Provision of study material
Angelique Bordey: Other (financial support and instruction of student)
Peng Jin: Concept and design, data analysis and interpretation, financial support, final approval of manuscript.
Xinyu Zhao: Concept and design, data analysis and interpretation, financial support, manuscript writing, final approval of manuscript.

Keywords

miR-137; microRNA; neural stem cells; adult neurogenesis; dendritic development; neuronal maturation

INTRODUCTION

In both embryonic and adult brains, neurogenesis is initiated from the neuronal fate specification of neural stem cells. To function properly, new neurons have to integrate into appropriate neural networks and establish correct communication with other neurons. A critical step in development is neuronal maturation, which is characterized by dendritic and axonal growth, synaptogenesis, neuronal and synaptic pruning, and modulations of neurotransmitter sensitivities [1, 2]. The process of neuronal maturation is regulated by complex mechanisms that are still unclear, and deficits in this step are evident in many neurodevelopmental disorders such Rett Syndrome, Fragile X syndrome, and autism, etc [3].

MicroRNAs (miRNAs) are small non-coding RNAs that can modulate gene expression at the post-translational level by targeting messenger RNA (mRNA), which leads to either reduced translation efficiency or cleavage of the target mRNAs. miRNAs are known to be involved in many cellular processes, such as proliferation, differentiation, apoptosis, and metabolism [4–7]. Despite the fact that 70% of detectable miRNAs are expressed in the brain, where half that number are either brain specific or enriched [8]. There have been few functional studies of miRNA in the nervous system. Recent evidence has shown that many miRNAs act locally at the neuronal dendritic spines [9, 10]. Both miR-134 and miR-138 are known to regulate dendritic patterning and spine morphogenesis by regulating protein translation at the synapse [11–13]. In addition, brain-specific miR-124 is localized at presynaptic terminal of Aplysia and regulates synaptic plasticity by regulating transcription factor CREB [14]. Recently, a neuronal activity-dependent miRNA, miR-132, is found to regulate dendritic development by targeting a Rho family GTPase-activating protein, p250GAP [15]. Therefore, small noncoding miRNA pathways could be an important and novel mechanism regulating mammalian neurodevelopment.

In this study we show that a neuron-enriched miRNA, miR-137, has a significant role in the phenotypic maturation and dendritic morphogenesis of young neurons. We establish that miR-137 regulates the translation of the mouse homolog of Drosophila Mind bomb 1 (Mib1), an ubiquitin ligase known to be important for neurogenesis and neurodevelopment [16–18]. Finally, we show that exogenously expressed Mib1 can partially rescue the phenotypic deficits associated with miR-137 overexpression. These data suggest that functional interaction between miRNA and Mib1 plays an important modulatory role in neuronal development.

MATERIALS AND METHODS

Animals

All animal procedures were performed according to protocols approved by the University of New Mexico Animal Care and Use Committee. Wildtype C57/B6 mice were used for in vivo and in vitro studies. For histological analyses, mice were euthanized by intraperitoneal injection of sodium pentobarbital. Mice were then perfused with saline followed by 4% PFA. Brains were dissected out, post-fixed overnight in 4% PFA, and then equilibrated in 30% sucrose. Forty-micrometer brain sections were generated.

Isolation and differentiation of adult hippocampal neuroprogenitors

Adult hippocampal neuroprogenitors (A-94-NSCs) was characterized previously and NSC proliferation and differentiation were carried out as described [19]. [20].

Relative quantification of mature miRNAs by Taqman miRNA real-time PCR

Mature miRNA expression was assayed using Applied Biosystems' TaqMan microRNA assays or individual TaqMan miRNA assays) were performed according to protocols provided by the vendor [21]. Detailed methods are provided in the Supplemental Data. Undifferentiated A94 NSCs were run in parallel with lineage specific differentiated A94 NSCs as paired samples. Data from the replicate experiments on undifferentiated A94 NSCs was then pooled and a single analysis of miRNA expression in each NSC lineage relative to undifferentiated NSCs was determined within the SDS v1.2 RQ manager to obtain the reported values.

miRNA in situ hybridization

In situ hybridization on 10 μm thick serial cryosections was carried out as outlined previously with a few modifications [22]. For hybridization 0.1 μl of 25 μM DIG- or FITC-labeled LNA probe (Exiqon) was added to 100 μL hybridization buffer and applied to the tissue at 50–60 °C overnight (~20°C below the predicted melting temperature (T_m) of probe:miRNA). Slides were mounted in Aquamount and visualized using confocal microscopy. Detailed methods are provided in the Supplemental Data

Nucleic acid and expression constructs

Control miRNA (miR-Con), miR-137, anti-miR-137, and anti-miRNA control (anti-miR-Con) were purchased from either GenePharma (Shanghai, China) or Ambion (AM17100, AM17110, AM17000, and AM17010, Austin, TX). Mib1 expression plasmid was described previously (Choe et al., 2007). Mib1 shRNA and non-silencing control was purchased from Qiagen/SABiosciences (KM26177G). Lentivirus-sh-Control was created by cloning the SureSilencing non-silencing control shRNA cassette into the HpaI and ClaI sites of lentiviral vector. The generation and validation of this Lentivirus-sh-Control was described previously [23, 24]. PCR based generation of the miR-137 shRNA driven by a U6 Pol III promoter was done as described in our publications [23, 24]. Detailed methods and sequences of primers are provided in the Supplemental Data. Retroviral vector expressing both miR-137 and eGFP was engineered by deleting the original HpaI and ClaI sites in the CAG-EGFP vector [25, 26] and inserting new HpaI and ClaI sites 5′-upstream from the CAG promoter. The sh-miR-137 or the sh-miR-Control cassette were digested from Lentiviral vectors (see above) and inserted between the HapI and ClaI sites of the retroviral vectors. The lentiviral and retroviral vectors expressing sh-miR-137 or sh-miR-Control were then verified by sequencing.

Production of retrovirus expressing miR-137 and in vivo retroviral grafting

Retrovirus production was performed as described previously [25, 26]. Detailed methods are provided in the Supplemental Data.

Maturation analysis of retroviral labeled new neurons

Immunohistochemistry and confocal imaging analysis on floating brain sections were carried out as described [25]. Floating brain sections containing eGFP+ cells were selected for staining and matched by DG region. The primary antibodies used were chicken anti-GFP (Invitrogen, #A10262), mouse NeuN (Chemicon, MAB377), and rabbit anti-doublecortin (DCX, Cell Signaling, #4604). The secondary antibodies used were anti-

chicken Alexa Fluor 488 (Invitrogen, #A11039), goat anti-mouse Alexa Fluor 647 (Invitrogen, #A21236), and goat anti-rabbit Alexa Fluor 568 (Invitrogen, #A11036).

For dendritic branching analysis on 300 μm thick floating brain sections, GFP+ neurons were imaged on a LSM 510 confocal with a 20x/oil objective. Z-stacks of GFP+ dendrites were captured at 8μm intervals and the dendrites and the cell body of single GFP+ neurons were analyzed by Neurolucida software (MicroBrightField, Inc.). Roughly 30–50 neurons per DG were traced. Data were extracted for Sholl analysis, total dendritic length, branch number, and dendritic end number for each GFP+ neuron. Neurons were selected for analysis based on expression of GFP throughout the cell body and its processes. Cells were excluded if they exhibit excessive overlapping with adjacent GFP expressing neurons, their morphology is not intact, they have membrane varicosities, or they show signs of cell death such as compacted chromatin structure revealed by DAPI staining.

For dendritic spine density analyses and quantification of stage-specific neuronal markers, 1-in-3 of 40 μm floating brain sections containing eGFP+ cells (120 μm apart, approximately 8 brain sections) were used for immunohistological staining using established protocols [25]. For the dendritic spine analysis above, the spine width was also manually measured as the distance of a straight line drawn across the widest part of the spine head using Image-J software (NIH Image).

Isolation of primary neurons from mouse embryos and transfection of cultured neurons

Hippocampwal neurons were isolated from E17.5 fetal mice, and grown as described previously [27, 28]. Hippocampal neurons from wildtype E17.5 fetal mice were grown as dispersed mixed cell cultures, as established by the Wilson lab [28]. Hippocampal neurons were transfected on day 4 (DIV 4) as they are undergoing dendritic and axonal morphogenesis during this time. Transfection was performed as described [27]. 48hours after transfection, the neurons were fixed and stained as described below. Transfection efficiencies were 1–2%.

Morphological analysis of transfected neurons

Immunostaining of transfected neurons was performed as previously described [20, 23, 25, 29]. The primary antibody used was MAP2ab (mouse, 1:500, Sigma). The secondary antibody used was Cy3 (donkey anti-mouse, 1:500, Sigma). Low transfection efficiencies (1–2% neurons) permit imaging and quantification of single GFP expressing neurons. GFP expressing neurons were imaged with an Olympus BX51 upright microscope with 20x/oil immersion lens, a motorized stage, and digital camera. Dendritic traces were performed in real time using Neurolucida (MicroBrightField, Inc.) image analysis software. The axon is identified using Map2 staining where the only process not positive for Map2 is the axonal process [30].

3′-UTR dual luciferase assays of miR-137 target mRNA

3′-UTR sequences of candidate mRNAs were PCR amplified directly from proliferating aNSC first strand cDNA generated from 5 μg TRIZOL-isolated total RNA using oligo-dT SuperScript III reverse transcription according to the manufacturer's protocol (Invitrogen, Cat. #1808-093). These primer sequences are available upon request. All primers were designed incorporating XhoI and NotI restriction sites and 4 bp of extra random sequence to aid in restricting digestion. XhoI- and NotI-digested PCR products were cloned into XhoI- and NotI-digested psiCHECK-2 dual luciferase vector (Promega, Cat# C8021) and were later transferred by XhoI/NotI double digestion and T4 DNA ligation into a pIS2 renilla luciferase vector modified with the addition of an XhoI restriction site and deletion of the SpeI restriction site. miR-137 target site deletion was done using the QuickChange Site-

Directed Mutagenesis Kit (Stratagene, Cat. #2000518) to delete UUCGUUAU. Briefly, E17 hippocampal neurons were cultured (as described above), and co-transfected by Lipofectamine 2000 with pIS2 Renilla luciferase vector containing the *Mib1* 3′UTR, pIS0 firefly luciferase as a transfection control, and miR-Con, miR-137, anti-miR-137, or anti-miR-Con. All co-transfections used a total of 1 μg of plasmid DNA and 50ng of shRNA. At 48 h after transfection, the cell culture medium was removed and cells were lysed with 20 μl of 1X passive lysis buffer at room temperature for 15 min and luciferase expression was detected using the Dual-Luciferase Reporter 1000 System (Promega, Cat# E1980) per the manufacturer's protocol. R-luc activity was normalized to F-luc activity to account for variation in transfection efficiencies, and miR-137–mediated knockdown of R-luc activity was calculated as the ratio of normalized R-luc activity in the U6-miR-137-shRNA treatments to normalized R-luc activity in the U6-neg-shRNA treatments. Luciferase experiments were repeated at least three times.

Production of lentivirus and infection of E17 hippocampal neurons

Lentiviruses were produced as described previously [23, 29, 31]. To study the effects of miR-137 on development of dendrites in cultured neurons, 1:1 solution of virus containing supernatant and Neurobasal A medium (Invitrogen) supplemented with 25 nM glutamate, 0.5 mM L- glutamine, and 1% antibiotics was added to the neurons 1 day after plating. After 24hours, the medium was replaced with fresh virus containing solution described above, and was incubated for an additional 24 hours. Infected neurons were collected in cell lysis buffer for western blot analysis.

Western blot analysis

Protein samples were separated on SDS-PAGE gels and then transferred to PVDF membranes (Millipore). Membranes were processed following the ECL Western Blotting protocol (GE Healthcare, Cat #RPN2106). Anti-Mib1 antibody (M20a) [16] were used at a 1:1000 dilution. HRP-labeled secondary antibodies were obtained from Sigma (A0545). For loading controls, membranes were stripped and reprobed with the antibody against GAPDH (Ambion AM4300).

Statistical analysis

All statistical analyses were performed using unpaired, two-tailed, Student's t-test. The data bars and error bars indicate mean ± standard error mean. (s.e.m). Scholl analysis was analyzed using a multivariate analysis of variance (MANOVA) using SPSS statistical software (SPSS version 17, SPSS Inc., Chicago, Ill, USA).

RESULTS

miR-137 is enriched in neurons

To identify lineage specific miRNAs that may regulate development and function of neurons in the postnatal hippocampus, we profiled mature miRNA expression in adult hippocampal neuroprogenitors (A94-NSCs) differentiated into either neuronal or astrocytic lineages and compared the miRNA profile in undifferentiated A94-NSCs (Supplemental Figure S1A and B). We then quantitatively identified miRNAs that were enriched specifically in the neuronal lineage relative to the astrocytic lineage (Figure 1A). Several miRNAs, particularly miR-185, 27b, 182, 137, 29b, 132, and 146, showed enrichment in neurons, but not astrocytes or undifferentiated NSCs; among these miRNAs, miR-137 was previously found to be enriched in synaptosomes isolated from rat forebrains [12, 32]. We further confirmed that the expression levels of miR-137 increased during neuronal differentiation of A94-NSCs (Figure 1B), and miR-137 expression levels were significantly higher in isolated

primary neurons compared with aNSCs (Figure 1C). The highly enriched expression of miR-137 in the neuronal lineage suggests that it may have important functions in neuronal development.

miR-137 is known to be expressed in the brain and enriched at the synaptic compartment [12, 32]. We reasoned that if miR-137 is indeed a mediator of neurodevelopment and function, it should be expressed in neurons of the adult hippocampus, which is a region of the brain exhibiting significant plasticity and continuous production of new neurons. Thus we chose to examine the cellular localization of miR-137 in the adult hippocampus. Hybridization with an miR-137-specific probe showed an enrichment of miR-137 within the dentate gyrus (DG) and molecular layer of the hippocampus compared with miR-1, a miRNA that is expressed at low levels in the central nervous system (CNS) (Figure 1D and E). Together, these data and the published literature [10, 12, 32] suggest that miR-137 may play functional roles in neurons, perhaps during the formation of connectivity between neurons in the hippocampus.

miR-137 regulates dendritic development and phenotypic maturation of new neurons in vivo

Recently, miRNAs were found to be expressed at the synapse and play an important role in dendritic patterning and spine morphogenesis [9, 11, 12]. To determine whether elevated miR-137 levels in neurons can affect neuronal maturation and dendritic morphogenesis, we overexpressed miR-137 in newborn cells of the adult DG using retrovirus-mediated gene delivery [25]. This method, referred to as the single-cell genetic approach [33, 34], makes use of recombinant retroviruses capable of specifically infecting dividing cells (Figure 2A). Because postnatal neurogenesis persists in the adult hippocampus, this method allows us to deliver a transgene specifically to newborn cells in the DG and perform a detailed morphological and phenotypic analysis on these newly generated neurons [25, 26, 33]. Using stereotaxic microinjection surgery, we grafted retrovirus expressing both eGFP and small hairpin miR-137 (sh-miR-137) into one hemisphere of the adult mouse DG, and injected a retrovirus carrying nonsilencing small hairpin control (sh-Con) into the contralateral hemisphere of the same animal (Figure 2A and B). At 4 weeks post-injection (4wpi), one cohort of injected animals was used to generate thick (300-μm) sections, which preserves the dendritic arborization of eGFP-positive neurons and enables extensive morphological analysis. Individual eGFP-expressing neurons in these sections were imaged using confocal microscopy. To precisely evaluate the dendritic complexity of eGFP+ neurons, we reconstructed the eGFP+ dendritic arbor in 3 dimensions, rather than the traditionally flattened 2 dimensions, for image analysis using the Image Stack Module of Neurolucida analysis software (MicroBrightField, Inc.) (Figure 2C and D, Supplemental Figure S2, Supplemental movie). Since previous reports have indicated that miR-137 has no affect on dendritic spine volume [12], we performed quantitative analysis using established parameters for assessing neuronal dendritic development [26, 35]. Sholl analysis indicated that miR-137-overexpressing neurons exhibited significantly reduced dendritic complexity compared to sh-Control-expressing neurons ($F(1,65) = 8.78$, $p = 0.004$, multivariate analysis of variance) (Figure 2E). In addition, miR-137-overexpressing neurons exhibited significantly reduced average dendritic length ($n = 3$ animals, $p < 0.05$), number of nodes (branch points) ($n = 3$, $p < 0.05$), and number of dendritic endpoints ($n = 3$, $p < 0.05$) compared with young neurons expressing sh-Control (Figure 2F–H).

Dendritic spine density increases as neurons mature, making the spine density a good indicator of neuronal maturation [26, 36]. On the other hand, altered spine density is a common characteristic of abnormal synaptic development in a variety of neurological disorders such as Fragile-X and Rett syndrome [3, 25]. We therefore used another cohort of virus-injected animals to generate 40-μm thin sections for dendritic spine analysis. To

determine whether overexpression of miR-137 leads to deficits in spine morphogenesis, we analyzed the dendritic spine density of newborn GFP-expressing DG granule neurons at 4 weeks post-injection, a time at which labeled new neurons are believed to exhibit the dendritic morphology of mature neurons [26, 34, 36]. To maximize consistency of our analyses, we focused on dendritic fragments 25–100 um from the cell body of each eGFP+ neuron. To quantify spine density, we counted the number of spines protruding from the dendrite within each 10-μm segment of dendrites. Quantitative analysis showed that miR-137-overexpressing neurons exhibited a 17% reduction in dendritic spine density compared with sh-Control-expression neurons ($n = 3$, $p < 0.01$) (Figure 2I–K). The widths of dendritic spines in miR-137-overexpressing neurons were no different from sh-Control-overexpressing neurons (Supplemental Figure S3).

New neurons in the DG express development stage-specific markers that define their maturation (Figure 3A) [37, 38]. Using immunocytochemistry for doublecortin (DCX, an immature neuronal marker) and neuronal nuclear antigen (NeuN, a mature neuronal marker) immunostaining, new neurons in the DG were categorized into 3 subpopulations: immature neurons (DCX+ only), transitioning neurons (DCX+ and NeuN+), and mature neurons (NeuN+) [25, 39]. We then determined whether new neurons overexpressing miR-137 had a developmental phenotype that could be measured by the expression of stage-specific markers. Thus, we analyzed retrovirus-labeled newborn neurons at 4 weeks post-injection, a time when many virus-labeled cells have differentiated into mature neurons (Figure 3A–C). We found that miR-137-overexpressing cells differentiated into fewer eGFP+ neurons (either DCX+eGFP+ and/or NeuN+eGFP+ cells) in general compared with sh-Control-overexpressing cells (Supplemental Figure S3). We then quantified the proportion of each type of neuron among total eGFP+ neurons. The results summarized in Figure 3D show that neurons overexpressing miR-137 displayed a significant difference in the proportion of immature vs. mature neurons compared with neurons overexpressing control (sh-Con). Specifically, miR-137-overexpressing neurons had an 80% decrease in the proportion of mature neurons (NeuN+, $n = 3$, $p < 0.05$) compared with control. Additionally, there was a 19% decrease in the proportion of transitioning neurons (NeuN+/DCX+, $n = 3$, $p > 0.05$) and a 62% increase in the proportion of immature neurons (DCX+, $n = 3$, $p = 0.05$) compared with control. Therefore, this indicates that elevated levels of miR-137 alter the sequential events leading to the development of a mature DG granule neuron. Taken together, these in vivo data suggest that increased expression of miR-137 in newborn neurons results in decreased dendritic development.

miR-137 regulates neuronal dendritic development in vitro

Since retrovirus infects only dividing cells, overexpression of miR-137 in dividing neuroprogenitors may affect initial neuronal differentiation, which might indirectly inhibit neuronal maturation. To investigate whether miR-137 overexpression affects neuronal maturation independent of its effect on the neuronal differentiation of neuroprogenitors, we turned to a well-established in vitro cultured primary neuron system and used both gain-of-function and loss-of-function methods. Hippocampal neurons serve as a good model for studying molecular mechanisms controlling dendritic and spine development, because they form elaborate dendritic trees, functional synapses, and they can respond to both chemical and electrical stimulations [40–42]. We isolated neurons from the hippocampi of E17.5 mouse embryos and plated them into serum-free medium to limit astrocyte proliferation. To modulate miR-137 expression, we overexpressed miR-137 using two different gain-of-function assays. First, we expressed miR-137 as a small hairpin RNA plasmid using a lentiviral vector that also expresses eGFP (Figure 4A) [29]. Second, we cotransfected neurons with miR-137 synthetic double-stranded RNA and an eGFP expression plasmid.

Concurrently, we performed a loss-of-function assay to knock down endogenous miR-137 in cultured hippocampal neurons using a 2′-O-methylated antisense oligonucleotide.

At 48 hours post-transfection, eGFP-expressing neurons were imaged, and the morphology of the soma, dendrites, and axons were manually traced and measured using Neurolucida (MicroBrightField, Inc.) image analysis software (Figure 4B and C). Transfected eGFP+ neurons had clearly identifiable dendrites and axons, and axons were distinguished from dendrites by two characteristics: axons are the longest among all processes and have negative staining for MAP2, a somatodendritic marker [30]. The morphology of cultured hippocampal neurons is not as uniform as developing neurons in the DG of the hippocampus, which may account for the variability we saw in neuronal morphometry. However, the morphological differences between neurons expressing miR-137 and controls were apparent (Supplemental Figure S4A, B). Neurons transfected with plasmid expressing sh-miR-137 had a significantly reduced dendritic complexity ($F(1,52) = 5.15$, $p < 0.05$ multivariate analysis of variance) (Figure 4D) and 23% reduction in total dendritic length ($n = 3$, $p < 0.05$) (Figure 4E) compared with sh-Control-transfected neurons. Consistent with this result, neurons transfected with synthetic miR-137 also showed a 23% reduction in dendritic length and reduced dendritic complexity compared with miR-Control-transfected neurons ($n = 3$, $p < 0.01$) (Figure 4F and G). On the other hand, neurons transfected with a specific inhibitor of miR-137 (anti-miR-137) had increased dendritic complexity ($F(2,51) = 3.58$, $p = 0.036$ multivariate analysis of variance) (Figure 4F) and a significant 25% increase in total dendritic length ($n = 3$, $p < 0.01$) (Figure 4G) compared with control anti-miR (anti-miR-Con)-transfected neurons. The total number of dendritic ends and nodes had a similar trend of a reduction in neurons transfected with miR-137 and an increase in anti-miR-137-transfected neurons; although these differences did not reach statistical significance (Supplemental Figure S4C and D). These loss-of-function and gain-of-function data in primary neurons further support our in vivo observation that high levels of miR-137 inhibit neuronal dendritic development.

Mind Bomb-1 is a Translational Target of miR-137

To determine how miR-137 affects dendritic morphology during neuronal development, we first took a bioinformatic approach to identify the potential mRNA targets of miR-137. We referenced TargetScan 4.1, PicTar, and miRanda to compile a set of potential candidate targets [43–45]. Next, we selected a subset of targets for further analyses based on 3 criteria: conservation, context score of target “seed sequences,” and known relevance to dendritic morphogenesis and neuronal development. Among the top candidate miR-137 targets are a mouse homolog of Drosophila mind bomb 1 (Mib1), histone H3K27 methyltransferase Ezh2, EphA7, and chromatin modulator NcoA3 (Table S1). We first cloned the 3′-untranslated region (3′-UTR) of these four candidates containing the predicted miR-137 target site from mouse cDNA into a Renilla luciferase (R-luc) reporter construct (see Figure 5B for example). This allowed us to assess protein translation of these targets regulated through their 3′-UTR. This 3′-UTR R-luc constructs along with a firefly luciferase (f-luc) control plasmid were cotransfected into HEK 293 cells. We found that miR-137 could repress the translation of luciferase through these 3′-UTR. Then we selected the expression plasmids of the top two candidates, Mib-1 and Ezh2, to transfect into primary neurons. We found that Mib1, but not Ezh2, could promote dendritic morphogenesis, similar to the effect of anti-miR-137. Mind bomb 1 (Mib1) was a particularly interesting candidate because it was previously shown to be enriched in the postsynaptic compartment by mass spectrometry [16, 46]. In addition, in our initial functional screening by overexpressing these candidate targets in cultured primary neurons, Mib1 demonstrated the most dramatic effect on promoting neuronal dendritic length (data not shown). We therefore decided to further investigate whether Mib1 is a functional target of miR-137. To further test whether miR-137

could target Mib1, we cloned the 3′-untranslated region (3′-UTR) of *Mib1* containing the predicted miR-137 target site, from mouse cDNA into a Renilla luciferase (R-luc) reporter construct (Figure 5B). This allows us to assess Mib1 protein translation regulated through its *Mib1* 3′-UTR. This 3′-UTR R-luc construct along with a firefly luciferase (f-luc) control plasmid were cotransfected into cultured primary neurons. We found that overexpression of miR-137 suppressed over 50% of the R-luc activity in primary neurons at 48 hours post-transfection ($n = 7$, $p < 0.001$) (Figure 5C). On the other hand, transfected anti-miR-137 led to a 28% increase in R-luc activity compared with the anti-miR control (anti-miR-Con, $n = 3$, $p < 0.05$) (Figure 5D). To further validate the interaction between miR-137 and its target *Mib1* 3′-UTR, we mutated the seed sequence of miR-137 located within the *Mib1*-3′-UTR reporter (Figure 5,B lower panel). This mutation substantially alleviated the miR-137-mediated suppression of luciferase activity, suggesting that the action of miR-137 is specific to the miR-137 seed region within the *Mib1*-3′-UTR ($n = 5$, $p < 0.001$) (Figure 5E).

To investigate the effect of miR-137 on endogenous Mib1 expression in neurons, we used the lentivirus expressing sh-miR-137 (Figure 4A) to infect cultured primary neurons. Lentivirus transduction allows us to achieve relatively high expression efficiency (~50%) in mouse primary neurons (Figure 5F). Neurons infected by sh-miR-137 expressing virus had a 13% decrease in endogenous Mib1 expression compared with neurons infected by control virus (sh-Con, $n = 3$, $p < 0.05$) (Figure 5G). Taken together, these data suggest that miR-137 regulates the protein expression of Mib1 through the 3′-UTR of Mib1.

Expression of Mib1 rescues the miR-137-mediated reduction in dendritic complexity

Since we have confirmed that miR-137 targets Mib1, we performed additional experiments to determine whether Mib1 could rescue the miR-137 overexpression-induced reduction in dendritic complexity. We showed that overexpression of Mib1 led to significant increases in both dendritic length ($n = 5$, 41% +/−0.12 SEM, $p < 0.01$) and dendritic complexity ($F(1,36) = 23.00$, $p < 0.001$) compared with control vector-transfected neurons (Figure 6A and B). On the other hand, using a specific small hairpin RNA (shRNA) against Mib1 (Supplemental Figure S6), we also showed that acute knockdown of Mib1 led to a significant decrease in both dendritic length (37.5% +/−0.09 SEM, $n = 3$, $p < 0.05$) and dendritic complexity ($F(1,47) = 49.00$, $p < 0.001$) compared with control shRNA-transfected neurons (Figure 6A and 6B). Then, we cotransfected neurons with Mib1 expression plasmid and a synthetic miR-137 and show that Mib1 overexpression partially rescued the miR-137-mediated reduction both in dendritic length ($n = 4$, 6% difference between “Mib1+miR-137” and “Control GFP”, 33% difference between “Mib1+miR-137” and “miR-137”) (Figure 6A) and in dendritic complexity ($F(1,35) = 18.51$, $p < 0.001$) (Figure 6C). These data suggest that miR-137 regulates dendritic morphogenesis in developing neurons, at least in part, by translational regulation of Mib1 (Figure 6D).

DISCUSSION

The potential functions of miRNAs acting locally at the neuronal dendritic spines are just beginning to be explored [10]. Several miRNAs are found to be localized and functioning in dendrites and synapses. Among them, miR-132 and miR-137 are both enriched in dendritic spines, but whereas miR-132 represses spine volume, miR-137 shows no effect on spine volume [12]. Therefore it is likely that individual miRNAs at the synapse play specialized roles in dendritic morphogenesis and synaptic development. Although the specific mechanisms underlying miRNA regulation of neuronal development are not fully clear, current experimental evidence suggest that miRNAs can have functions during all stages of neuronal development, including neural stem cell proliferation, neuronal fate specification, neurite outgrowth, and spine development [47]. In the case of miR-137, we believe that it may play a dual role in neurogenesis. miR-137 is found to induce differentiation of adult

mouse neural stem cells as well as mouse oligodendroglioma-derived stem cells and human glioblastoma multiform-derived stem cells [32]. Studies from our lab have shown that miR-137 also plays a role in the proliferation and differentiation of adult neural stem cells by targeting histone H3K27 methyltransferase Ezh2 [48]. Interestingly, we found that miR-137 regulates dendritic morphogenesis by targeting Mib1, not Ezh2 (Supplemental Table S1). These studies suggest that miR-137 plays different roles during the early and late stages of adult neurogenesis in the hippocampus. Additionally, our ISH data (Figure 1) shows miR-137 expression is widespread in the DG, suggesting that miR-137 may function in both developing and mature neurons. In fact, Siegel et al have found miR-137 is one of the miRNAs enriched in the synpatosome postnatal mature neurons [12]. Interestingly, double ISH/immunohistochemistry shows miR-137 overlaps with presynaptic synapsin, indicating that miR-137 may also function in the pre-synaptic compartment, in addition to the dendritic and postsynaptic compartment. It is well known that local protein synthesis is important for synaptic transmission and plasticity. In mature neurons miR-137 may regulate the translation of a subset of proteins that are important for neuronal activity-dependent protein expression and synaptic plasticity, similar to what has been found for miR-132 [49]. Thus, an interesting question to pursue would be whether miR-137 can mediate neuronal activity-dependent dendritic development. It is also possible that miR-137 has effects on the maintenance and survival of neurons. One could speculate that miRNAs in the dendrite may participate in the regulation of local protein translation and modify synaptic plasticity at the synaptic compartment; however, a complete story of how miRNAs and their dendritic target mRNAs regulate dendritic morphogenesis and synaptic development has yet to be told and remains a critical area of future neurodevelopment studies.

The most challenging step in determining the function of miRNA is to identify their downstream mRNA targets. Based on bioinformatic databases, we know that each miRNA can have many potential mRNA targets, yet whether these predicted mRNA targets are functional in the context of miRNA-mediated gene regulation remains to be determined. However, only a small number of these predicted targets are true targets. In addition to Mib1, several additional miR-137 targets are strongly associated with neuronal development and synaptic function including Ezh2, EphA7, EphB2, NcoA3, Shank2, and Snap23. Even though some of these predicted targets did not show obvious functional rescue in our initial screening, we cannot rule out the possibility that miR-137 could function by modulating the translation of these genes to a lesser extent. Further experiments to identify additional miR-137 targets will give us a more complete picture of miR-137 function during neurodevelopment

An interesting question to pursue would be whether miR-137 can mediate neuronal activity-dependent dendritic development. Although neurons contain many potential targets of miR-137, we chose to follow ubiquitin ligase Mib1, because mass spectrometry has shown it to be enriched in the postsynaptic compartment [16, 46]. Mib1 was first cloned and studied in zebrafish [17], and the loss of Mib1 led to reduced lateral inhibition of Notch signaling, which in turn triggered changes in the number of progenitors and neuronal differentiation during zebrafish CNS development [17]. Mib1 is an E3 ubiquitin ligase and promotes ubiquitination and internalization of the Notch ligand Delta, leading to Notch pathway activation. In mammals, the function of Mib1 is not fully clear. In one study, Mib1 was found to activate the Notch pathway in embryonic mice, and Mib1 mutant mice exhibit deficits in neurogenesis and resemble mice lacking Notch signaling components [50]. Mib1 was also shown to be phosphorylated by PAR-1, resulting in Mib1 degradation and stimulation of neuronal differentiation in mammalian neuronal progenitors [18]. Similarly, Notch activation by Mib1-positive newborn neurons and intermediate progenitors in mice functions to ensure the maintenance of stem cell properties of radial glia during neurodevelopment [51]. A recent study shows that Mib1 inhibits dendritic development in

cultured rat cortical neurons [16]. The precise role of Mib1 in mammalian dendritic development is unknown; however, the importance of Mib1 in neuronal maturation is clearly demonstrated by both the published literature and our data.

The possible role of the E3 ubiquitin ligase Mib1 in neuronal maturation is intriguing, albeit vastly speculative. The ubiquitin pathway is best known for its role in marking target proteins for specific proteolysis by proteasomes; however, the ubiquitin pathway may also be involved in regulating the abundance of postsynaptic receptors [52]. A neuronal deficiency of UBE3A, an ubiquitin protein ligase involved in protein degradation, causes Angelman syndrome, which is characterized by severe mental retardation. In recent studies, UBE3A was found to localize to the synapse, and its deficiency resulted in abnormal dendritic and spine morphology [53, 54]. Mib1, on the other hand, seems to be involved in protein trafficking rather than protein degradation [17]. It may modify postsynaptic receptors or other regulatory molecules at the synapse and alter their intracellular localization, hence its involvement in dendritic patterning in developing and mature neurons. The fact that Mib1 can rescue the dendritic deficits associated with miR-137 overexpression further supports the positive effects of Mib1 on mammalian dendritic morphogenesis and its role as one of the downstream effectors of miR-137. Understanding this pathway may also shed light on the molecular mechanism underlying neurodevelopmental disorders associated with neuronal dendritic deficits.

SUMMARY

Our goal is to understand how noncoding miRNAs regulate development and functions of neurons. We have discovered a number of miRNAs that are enriched in neuronal lineage, relative to either astrocytic lineage or undifferentiated NSCs. Here we show that one of these miRNAs, miR-137, has an important modulatory role in dendritic morphogenesis during neuronal development both in vivo and in vitro. We find that overexpression of miR-137 using the “single-cell genetic approach” in newborn neurons of the adult hippocampus results in reduced dendritic complexity and spine density; however, since the single-cell genetic approach specifically targets proliferating cells prior to neuronal differentiation, we also confirmed that overexpression of miR-137 has the same effect on postmitotic cultured hippocampal neurons. Both overexpression and inhibition of miR-137 have significant but opposite effects on dendritic complexity. Therefore, our data indicate that proper expression of miR-137 is required for the normal dendritic development of hippocampal neurons.

Supplementary Material

Refer to Web version on PubMed Central for supplementary material.

Acknowledgments

Funding Acknowledgement: This work was supported by grants from NIH (MH080434, MH07897) and International Rett Syndrome Foundation (IRSF) to XZ; a Minority Supplement (MH080434) to RDS; Institutional Minority Student Development program (IMSD, NIH 2R25GM060201-09) to RLP; grants from NIH (NS051630 and MH076090) and IRSF to PJ.

We would like to thank the members of the Zhao and Jin Laboratories for their helpful discussions. We thank F. H. Gage for providing us the lentiviral vector and retroviral vector used to engineer the expression vectors for miR-137. Thanks to Michael C. Wilson and Lawrence Tafoya for providing training in neuronal culture methods. P.J. is supported by grants from the International Rett Syndrome Foundation and the NIH (NS051630 and MH076090). P.J. is the recipient of a Beckman Young Investigator Award, Basil O’Connor Scholar Research Award, and Alfred P. Sloan Research Fellow in Neuroscience. X.Z. is supported by grants from the International Rett Syndrome Foundation and the NIH (MH080434 and MH078972). X.L. was a recipient of the Autism Speaks Postdoctoral Fellowship. R.S. is supported by a Minority Supplement to NIH grant (MH080434). R.L.P. is supported by the NIH/GM060201-funded Initiatives to Maximize Student Diversity (IMSD) program.

References

1. Waites CL, Craig AM, Garner CC. Mechanisms of vertebrate synaptogenesis. Annu Rev Neurosci. 2005; 28:251–274. [PubMed: 16022596]
2. Webb SJ, Monk CS, Nelson CA. Mechanisms of postnatal neurobiological development: implications for human development. Dev Neuropsychol. 2001; 19:147–171. [PubMed: 11530973]
3. Fiala JC, Spacek J, Harris KM. Dendritic spine pathology: cause or consequence of neurological disorders? Brain Res Brain Res Rev. 2002; 39:29–54. [PubMed: 12086707]
4. Chang TC, Mendell JT. microRNAs in vertebrate physiology and human disease. Annu Rev Genomics Hum Genet. 2007; 8:215–239. [PubMed: 17506656]
5. Gangaraju VK, Lin H. MicroRNAs: key regulators of stem cells. Nat Rev Mol Cell Biol. 2009; 10:116–125. [PubMed: 19165214]
6. Liu C, Zhao X. MicroRNAs in Adult and Embryonic Neurogenesis. Neuromolecular Med. 2009
7. Carninci P, Kasukawa T, Katayama S, et al. The transcriptional landscape of the mammalian genome. Science. 2005; 309:1559–1563. [PubMed: 16141072]
8. Cao X, Yeo G, Muotri AR, et al. Noncoding RNAs in the mammalian central nervous system. Annu Rev Neurosci. 2006; 29:77–103. [PubMed: 16776580]
9. Lugli G, Torvik VI, Larson J, et al. Expression of microRNAs and their precursors in synaptic fractions of adult mouse forebrain. J Neurochem. 2008; 106:650–661. [PubMed: 18410515]
10. Smalheiser NR, Lugli G. microRNA regulation of synaptic plasticity. Neuromolecular Med. 2009; 11:133–140. [PubMed: 19458942]
11. Schratt GM, Tuebing F, Nigh EA, et al. A brain-specific microRNA regulates dendritic spine development. Nature. 2006; 439:283–289. [PubMed: 16421561]
12. Siegel G, Obernosterer G, Fiore R, et al. A functional screen implicates microRNA-138-dependent regulation of the depalmitoylation enzyme APT1 in dendritic spine morphogenesis. Nat Cell Biol. 2009; 11:705–716. [PubMed: 19465924]
13. Fiore R, Khudayberdiev S, Christensen M, et al. Mef2-mediated transcription of the miR379–410 cluster regulates activity-dependent dendritogenesis by fine-tuning Pumilio2 protein levels. EMBO J. 2009; 28:697–710. [PubMed: 19197241]
14. Rajasethupathy P, Fiumara F, Sheridan R, et al. Characterization of small RNAs in aplysia reveals a role for miR-124 in constraining synaptic plasticity through CREB. Neuron. 2009; 63:803–817. [PubMed: 19778509]
15. Wayman GA, Davare M, Ando H, et al. An activity-regulated microRNA controls dendritic plasticity by down-regulating p250GAP. Proc Natl Acad Sci U S A. 2008; 105:9093–9098. [PubMed: 18577589]
16. Choe EA, Liao L, Zhou JY, et al. Neuronal morphogenesis is regulated by the interplay between cyclin-dependent kinase 5 and the ubiquitin ligase mind bomb 1. J Neurosci. 2007; 27:9503–9512. [PubMed: 17728463]
17. Itoh M, Kim CH, Palardy G, et al. Mind bomb is a ubiquitin ligase that is essential for efficient activation of Notch signaling by Delta. Dev Cell. 2003; 4:67–82. [PubMed: 12530964]
18. Ossipova O, Ezan J, Sokol SY. PAR-1 phosphorylates Mind bomb to promote vertebrate neurogenesis. Dev Cell. 2009; 17:222–233. [PubMed: 19686683]
19. Palmer TD, Takahashi J, Gage FH. The adult rat hippocampus contains primordial neural stem cells. Mol Cell Neurosci. 1997; 8:389–404. [PubMed: 9143557]
20. Zhao X, Ueba T, Christie BR, et al. Mice lacking methyl-CpG binding protein 1 have deficits in adult neurogenesis and hippocampal function. Proc Natl Acad Sci U S A. 2003; 100:6777–6782. [PubMed: 12748381]
21. Lao K, Xu NL, Yeung V, et al. Multiplexing RT-PCR for the detection of multiple miRNA species in small samples. Biochem Biophys Res Commun. 2006; 343:85–89. [PubMed: 16529715]
22. Obernosterer G, Martinez J, Alenius M. Locked nucleic acid-based in situ detection of microRNAs in mouse tissue sections. Nat Protoc. 2007; 2:1508–1514. [PubMed: 17571058]

23. Barkho BZ, Munoz AE, Li X, et al. Endogenous matrix metalloproteinase (MMP)-3 and MMP-9 promote the differentiation and migration of adult neural progenitor cells in response to chemokines. Stem Cells. 2008; 26:3139–3149. [PubMed: 18818437]
24. Li X, Barkho BZ, Luo Y, et al. Epigenetic regulation of the stem cell mitogen FGF-2 by mbd1 in adult neural stem/progenitor cells. J Biol Chem. 2008 in press.
25. Smrt RD, Eaves-Egenes J, Barkho BZ, et al. Mecp2 deficiency leads to delayed maturation and altered gene expression in hippocampal neurons. Neurobiol Dis. 2007
26. Zhao C, Teng EM, Summers RG Jr, et al. Distinct morphological stages of dentate granule neuron maturation in the adult mouse hippocampus. J Neurosci. 2006; 26:3–11. [PubMed: 16399667]
27. Tafoya LC, Mameli M, Miyashita T, et al. Expression and function of SNAP-25 as a universal SNARE component in GABAergic neurons. J Neurosci. 2006; 26:7826–7838. [PubMed: 16870728]
28. Washbourne P, Thompson PM, Carta M, et al. Genetic ablation of the t-SNARE SNAP-25 distinguishes mechanisms of neuroexocytosis. Nat Neurosci. 2002; 5:19–26. [PubMed: 11753414]
29. Li X, Barkho BZ, Luo Y, et al. Epigenetic regulation of the stem cell mitogen Fgf-2 by Mbd1 in adult neural stem/progenitor cells. J Biol Chem. 2008; 283:27644–27652. [PubMed: 18689796]
30. Jugloff DG, Jung BP, Purushotham D, et al. Increased dendritic complexity and axonal length in cultured mouse cortical neurons overexpressing methyl-CpG-binding protein MeCP2. Neurobiol Dis. 2005; 19:18–27. [PubMed: 15837557]
31. Barkho BZ, Song H, Aimone JB, et al. Identification of astrocyte-expressed factors that modulate neural stem/progenitor cell differentiation. Stem Cells Dev. 2006; 15:407–421. [PubMed: 16846377]
32. Silber J, Lim DA, Petritsch C, et al. miR-124 and miR-137 inhibit proliferation of glioblastoma multiforme cells and induce differentiation of brain tumor stem cells. BMC Med. 2008; 6:14. [PubMed: 18577219]
33. Song H, Kempermann G, Overstreet Wadiche L, et al. New neurons in the adult mammalian brain: synaptogenesis and functional integration. J Neurosci. 2005; 25:10366–10368. [PubMed: 16280573]
34. van Praag H, Schinder AF, Christie BR, et al. Functional neurogenesis in the adult hippocampus. Nature. 2002; 415:1030–1034. [PubMed: 11875571]
35. Duan X, Chang JH, Ge S, et al. Disrupted-In-Schizophrenia 1 regulates integration of newly generated neurons in the adult brain. Cell. 2007; 130:1146–1158. [PubMed: 17825401]
36. Ge S, Goh EL, Sailor KA, et al. GABA regulates synaptic integration of newly generated neurons in the adult brain. Nature. 2006; 439:589–593. [PubMed: 16341203]
37. Ming GL, Song H. Adult neurogenesis in the mammalian central nervous system. Annu Rev Neurosci. 2005; 28:223–250. [PubMed: 16022595]
38. Zhao C, Deng W, Gage FH. Mechanisms and functional implications of adult neurogenesis. Cell. 2008; 132:645–660. [PubMed: 18295581]
39. Brown JP, Couillard-Despres S, Cooper-Kuhn CM, et al. Transient expression of doublecortin during adult neurogenesis. J Comp Neurol. 2003; 467:1–10. [PubMed: 14574675]
40. Goslin K, Banker G. Experimental observations on the development of polarity by hippocampal neurons in culture. J Cell Biol. 1989; 108:1507–1516. [PubMed: 2925793]
41. Fletcher EJ, Church J, MacDonald JF. Haloperidol blocks voltage-activated Ca2+ channels in hippocampal neurones. Eur J Pharmacol. 1994; 267:249–252. [PubMed: 8050486]
42. Okabe S, Collin C, Auerbach JM, et al. Hippocampal synaptic plasticity in mice overexpressing an embryonic subunit of the NMDA receptor. J Neurosci. 1998; 18:4177–4188. [PubMed: 9592097]
43. Lewis BP, Shih IH, Jones-Rhoades MW, et al. Prediction of mammalian microRNA targets. Cell. 2003; 115:787–798. [PubMed: 14697198]
44. Krek A, Grun D, Poy MN, et al. Combinatorial microRNA target predictions. Nat Genet. 2005; 37:495–500. [PubMed: 15806104]
45. John B, Enright AJ, Aravin A, et al. Human MicroRNA targets. PLoS Biol. 2004; 2:e363. [PubMed: 15502875]

46. Sheng M, Hoogenraad CC. The postsynaptic architecture of excitatory synapses: a more quantitative view. Annu Rev Biochem. 2007; 76:823–847. [PubMed: 17243894]

47. Liu C, Zhao X. MicroRNAs in adult and embryonic neurogenesis. Neuromolecular Med. 2009; 11:141–152. [PubMed: 19598002]

48. Szulwach KE, Li X, Smrt RD, et al. Crosstalk between microRNA and epigenetic regulation in adult neurogenesis. J Cell Biol. 2010:189. in press.

49. Vo N, Klein ME, Varlamova O, et al. A cAMP-response element binding protein-induced microRNA regulates neuronal morphogenesis. Proc Natl Acad Sci U S A. 2005; 102:16426–16431. [PubMed: 16260724]

50. Koo BK, Lim HS, Song R, et al. Mind bomb 1 is essential for generating functional Notch ligands to activate Notch. Development. 2005; 132:3459–3470. [PubMed: 16000382]

51. Yoon KJ, Koo BK, Im SK, et al. Mind bomb 1-expressing intermediate progenitors generate notch signaling to maintain radial glial cells. Neuron. 2008; 58:519–531. [PubMed: 18498734]

52. Burbea M, Dreier L, Dittman JS, et al. Ubiquitin and AP180 regulate the abundance of GLR-1 glutamate receptors at postsynaptic elements in C. elegans. Neuron. 2002; 35:107–120. [PubMed: 12123612]

53. Lu Y, Wang F, Li Y, et al. The Drosophila homologue of the Angelman syndrome ubiquitin ligase regulates the formation of terminal dendritic branches. Hum Mol Genet. 2009; 18:454–462. [PubMed: 18996915]

54. Dindot SV, Antalffy BA, Bhattacharjee MB, et al. The Angelman syndrome ubiquitin ligase localizes to the synapse and nucleus, and maternal deficiency results in abnormal dendritic spine morphology. Hum Mol Genet. 2008; 17:111–118. [PubMed: 17940072]

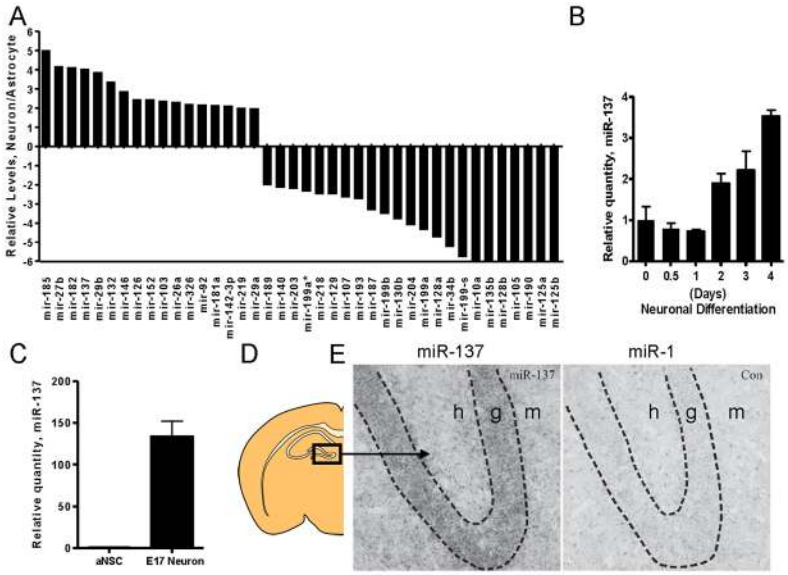

Figure 1.

miR-137 is enriched in neurons and is expressed in the dentate gyrus and the molecular layer of the hippocampus. (**A)** Identification of lineage specific miRNAs in A94-NSCs. Plotted are the ratios of RQ values determined by comparing A94-NSCs differentiated toward the neuron lineage to undifferentiated A94-NSCs over RQ values determined by comparing A94-NSCs differentiated toward the astrocyte lineage to undifferentiated A94-NSCs (Figure S1A and S1B). Ratios ≥8 were set to a value of 8. (**B)** miR-137 expression during neuronal differentiation of A94-NSCs for 0.5, 1, 2, 3, and 4 days (miR-137 expression calibrated to undifferentiated A94-NSCs, n=3, mean ± 95% CI). (**C)** Enrichment of miR-137 in E17 neurons as compared to mouse primary aNSCs (miR-137 expression calibrated to mouse primary aNSCs, n=3, mean ± SEM). (**D–E)** Hybridization with a miR-137-specific probe showed an enrichment of miR-137 within the DG and molecular layer of the hippocampus compared with miR-1, which is expressed at low levels in the CNS (h, hilus; g, dentate gyrus; m, molecular layer).

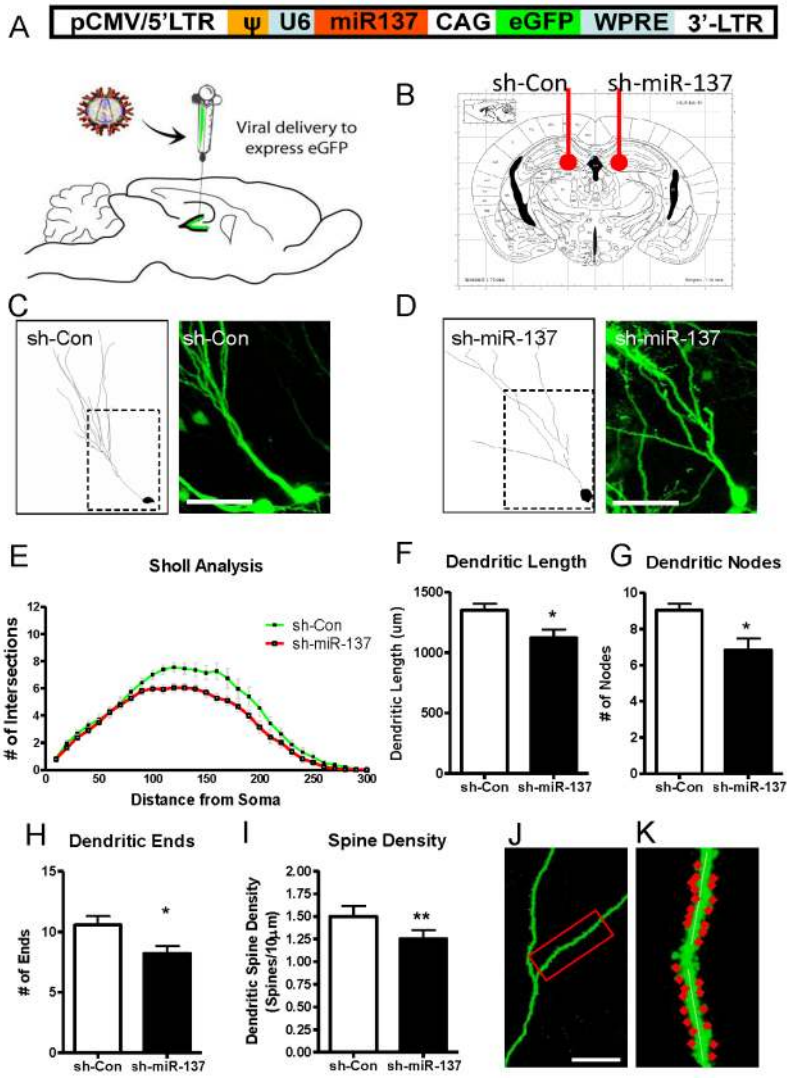

Figure 2.

miR-137 regulates dendritic development and phenotypic maturation of new neurons in vivo. (**A**) A schematic diagram showing the retroviral vector used for in vivo miR-137 expression. miR-137 (sh-miR-137) or control miR (sh-Con) was expressed as a short hairpin under U6 RNA Polymerase III promoter while eGFP was expressed under a chicken β-actin (CAG) promoter. (**B**) Schematic diagram showing that control virus (sh-Con) was injected into the left hemisphere, and retrovirus expressing miR-137 (sh-miR-137) was injected into the right hemisphere. (**C, D**) Confocal z-stacks showing eGFP-expressing neurons at 4 weeks post-injection (4 wpi) with representative traces from both the sh-Con (C) and sh-miR-137 condition (D) (scale bar = 50 μm). (**E**) Neurons overexpressing sh-miR-137 show reduced dendritic complexity compared with controls, as determined by Scholl analysis. (**F–H**) Neurons overexpressing sh-miR-137 show reduced dendritic length (F), number of nodes (branch points, G), and dendritic ends (H). (**I**) Neurons overexpressing sh-miR-137 show reduced dendritic spine density. (**J**) Confocal z-stacks showing eGFP-expressing dendrites (scale bar = 20 μm). **(K)** A representative dendritic segment used for spine density analysis (* = $p < 0.05$)

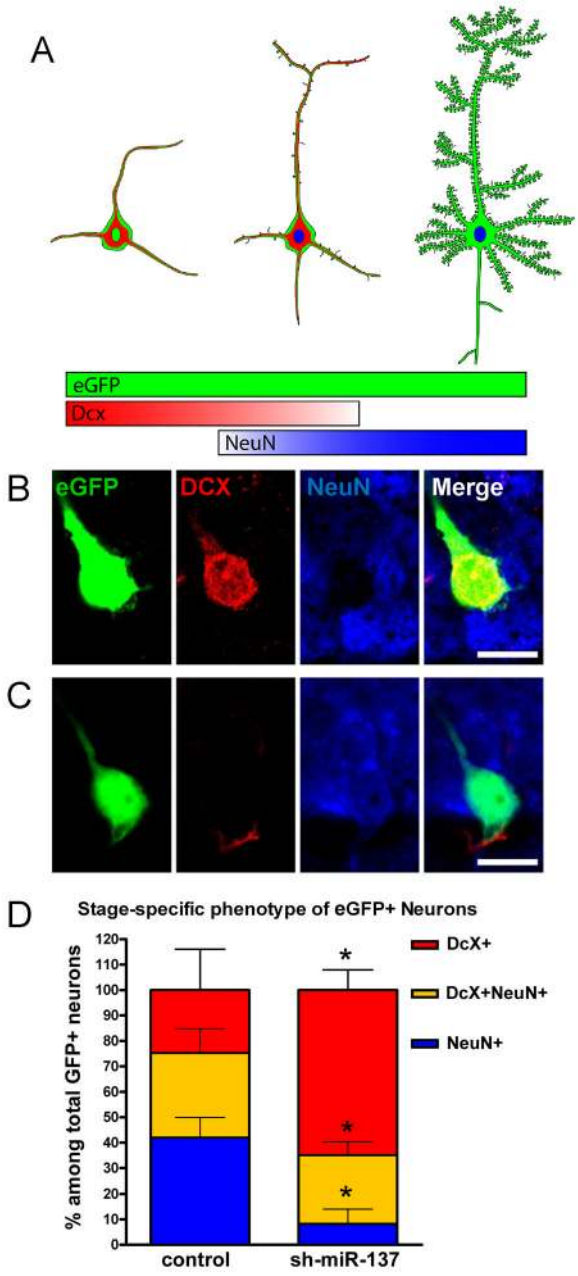

Figure 3.

Overexpression of miR-137 leads to altered neuronal maturation of new neurons in vivo. (**A**) Illustration showing the stage-specific neuronal markers that can be used to identify the maturation state of developing DG granule neurons. (**B, C**) Confocal images showing two representative eGFP-expressing neurons in the DG: a relatively immature eGFP neuron (B) expressed DCX (immature marker) but not NeuN (mature neuron) and a relatively mature eGFP+ neuron (C) expressed NeuN but not DCX. (**D**) The miR-137-overexpressing neuron population had decreased proportions of NeuN+ only (blue) mature neurons and of DCX+/NeuN+ (yellow) transitioning neurons, but increased proportion of DCX+ only (red) immature neurons compared with control (* = $p < 0.05$).

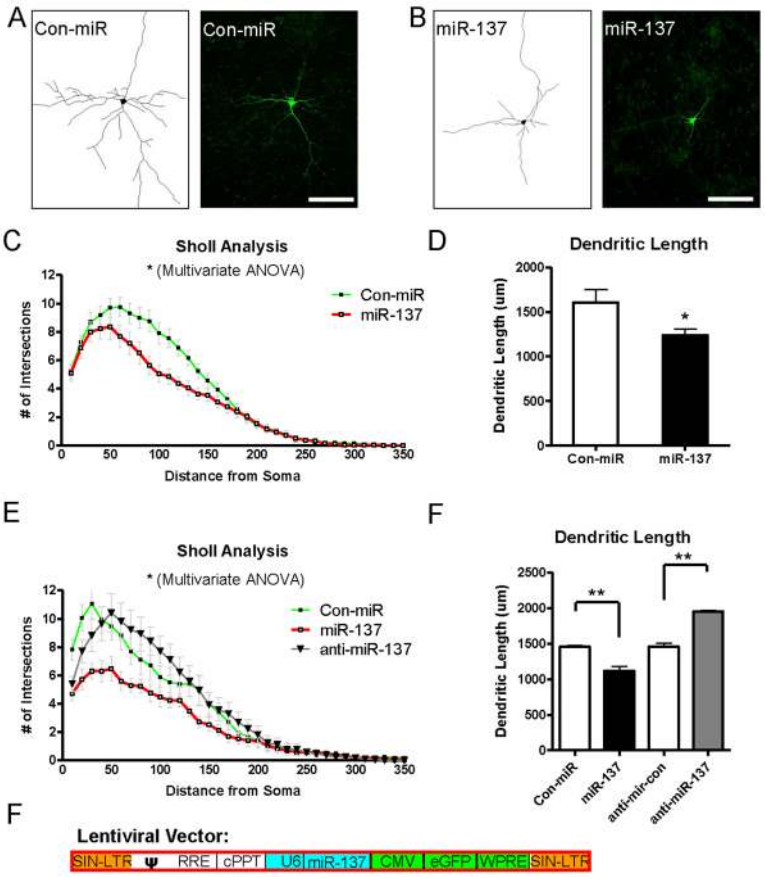

Figure 4.

miR-137 is important for dendritic development in vitro. **(A)** A schematic diagram showing the lentiviral vector used for miR-137 expression. miR-137 (sh-miR-137) or control miR (sh-Con) was expressed as a short hairpin under U6 RNA Polymerase III promoter while eGFP was expressed under a CMV promoter. **(B, C)**, E17 primary hippocampal neurons were transfected with lentiviral vectors expressing either control Con (B) or miR-137 (C), as well as eGFP. Single eGFP-expressing neurons were shown next to their representative traces (scale bar = 50 μm; 20x/oil). **(D)**, Scholl analysis showing neurons overexpressing sh-miR-137 had reduced dendritic complexity compared with neurons overexpressing sh-Control. **(E)**, Neurons overexpressing sh-miR-137 had reduced total dendritic length compared with controls. **(F)**, Scholl analysis showing that neurons overexpressing miR-137 had reduced dendritic complexity compared with controls, whereas neurons transfected with an anti-miR-137 had opposite effect. **(G)**, Neurons overexpressing miR-137 had reduced total dendritic length compared with neurons overexpressing miR-Control. On the other hand, neurons transfected with anti-miR-137 showed increased dendritic length compared to neurons transfected with anti-miR-Control. (*, $p < 0.05$, **, $p < 0.01$)

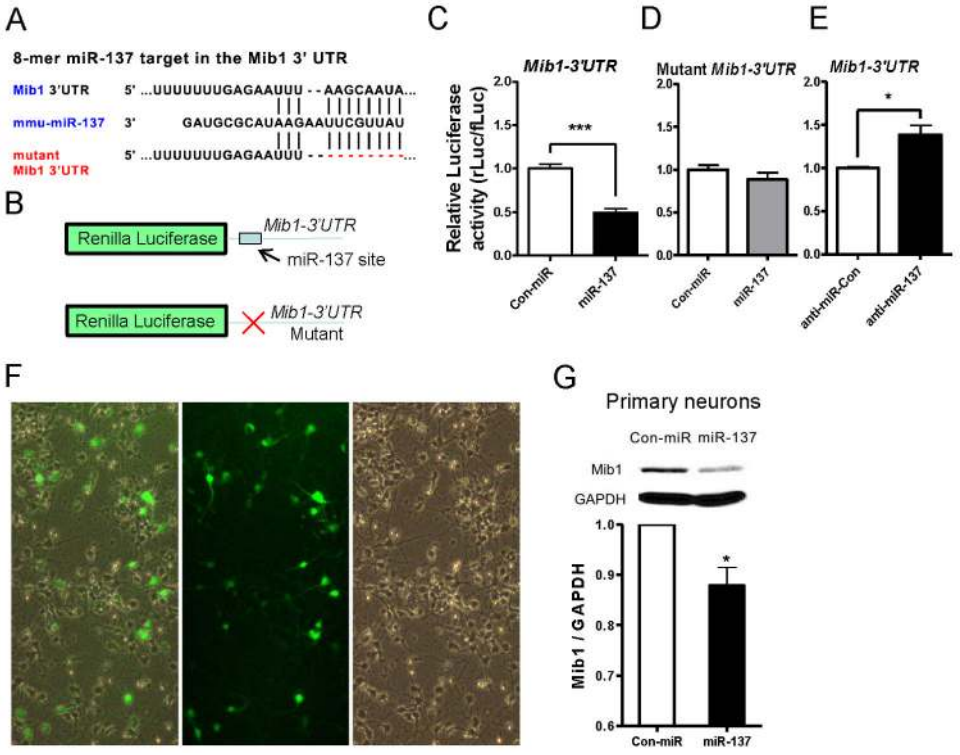

Figure 5.

Mib1 is a functional target of miR-137. (**A**) A miR-137 target site was found in the *Mib1* 3′ untranslated region (3′UTR) as predicted by TargetScan software. The Mutant *Mib1* 3′UTR used in B-E with miR-137 site deleted is shown. (**B**) Schematic diagram showing the predicted seed region where miR-137 is expected to bind the rLuc-*Mib1* 3′-UTR (upper), and the mutated version lacking the binding site for miR-137. (**C**) *Mib1*-3′-UTR–dependent expression of a Renilla luciferase reporter gene (R-luc) was suppressed by miR-137 over 50% in DIV6 primary neurons at 48 hours post-transfection ($n = 7$, $p < 0.001$). The 3′-UTR-dependent Renilla luciferase (R-Luc) activities were normalized to control firefly luciferase (f-Luc) activities in the result of miR-137 coexpression was calculated relative to the miR-Con in C–E. (**D**) The mutant *Mib1*-3′-UTR alleviated the miR-137-mediated suppression of luciferase activity, suggesting that the action of miR-137 is specific to the miR-137 seed region within the *Mib1*-3′-UTR ($n = 5$, $p < 0.001$). (**E**) *Mib1*-3′-UTR–dependent expression of R-Luc was enhanced 28% by anti-miR-137 ($n = 3$, $p < 0.05$). (**F**), 10x fluorescence and bright field images showing high infection efficiency of lentivirus expressing sh-miR-137 (also eGFP) in E17 primary cortical neurons. (**G**) Primary neurons infected with lentivirus expressing sh-miR-137 had reduced Mib1 protein expression compared with neurons infected with lentivirus expressing sh-Con at 48 hours post-infection. (*, $p < 0.05$; ***, $p < 0.001$)

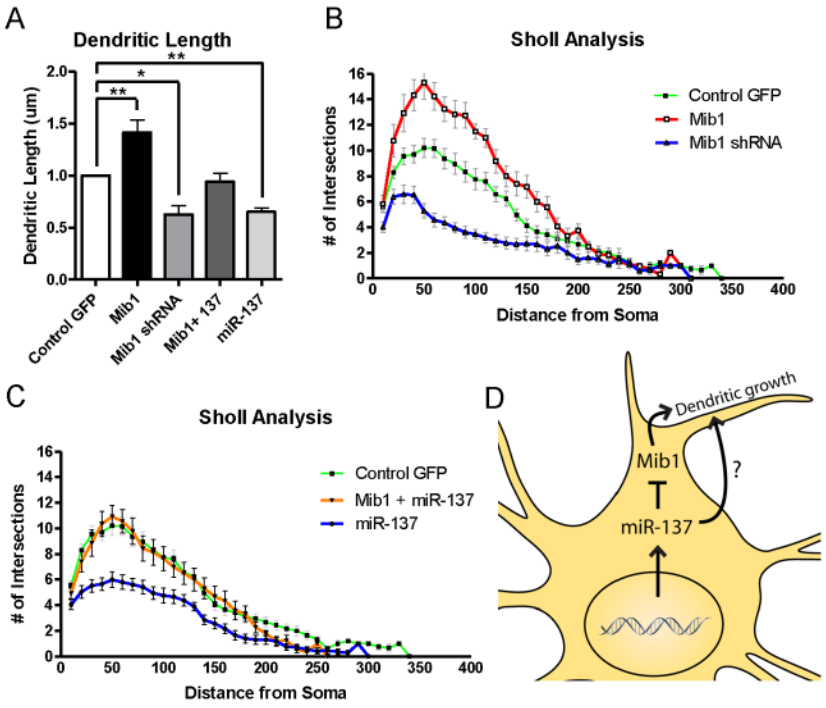

Figure 6.

Mib1 could rescue the neuronal maturation deficits associated with miR-137 overexpression in vitro. (**A**) Overexpression of Mib1 enhanced dendritic length, whereas acute knockdown of Mib1 (Mib1 shRNA) reduced dendritic length. Mib1 expression partially rescued the miR-137-mediated reduction in dendritic length in cultured primary neurons. (**B**) Overexpression of Mib1 enhanced the dendritic complexity of cultured neurons, whereas acute knockdown of Mib1 reduced dendritic complexity. (**C**) Mib1 could rescue the miR-137-mediated reduction in dendritic complexity ($F(1,35) = 18.51$, $p < 0.001$). (**D**) A hypothetic model illustrating that miR-137 may regulate dendritic morphogenesis in developing neurons, at least in part, by translational regulation of Mib1. (*, $p < 0.05$; **, $p < 0.01$; ***, $p < 0.001$).